7th International Conference on the Durability of Concrete Structures
20-22 May 2022
University of Jinan, Jinan, Shandong, China

Investigation on structural heritability and durability of high sulfate resistance Portland cement mortar modified by aluminum salt

Jun Xu[1], Haibo Fang[2], Haixia Zhang[2], Yang Yang[2], Yongtao Liu[2], Lingchao Lu[1,*]
[1]Shandong Provincial Key Lab. of Preparation and Measurement of Building Materials, University of Jinan, Jinan 250022, China
[2]The Second Construction Limited Company of China Construction Eighth Engineering Division

ABSTRACT

The essential hydration and hardened properties of high sulfate resistance Portland cement paste/mortar were investigated with $Al_2(SO_4)_3$ as admixture. Experiment results showed that that the addition of $Al_2(SO_4)_3$ promoted the hydration of HSRP cement pastes, and the hydration rate accelerated with the increase of the addition amount. The mechanical properties and chloride diffusion coefficient of cement mortar were obviously improved with 0.25% $Al_2(SO_4)_3$ addition . For instance, the compressive strength of AS0.25 cement mortars was 24.8% higher than AS0 samples and the chloride ion migration coefficient was 17.52% lower than AS0 samples after curing for 3-days.

1. INTRODUCTION

Marine concrete is a common man-made material in marine infrastructure. In view of the complex environment of sea water, the research on improving the mechanical properties and the corrosion resistance of marine concrete plays a major role in marine construction [1-4]. However, ordinary Portland cement reacted with sulfate ion in seawater to form expansive products, which causing concrete to crack [5,6]. Thus, High Sulfate Resistance Portland Cement (HSRPC) was proposed as alternative cementitious material by reducing the content of tricalcium aluminate(less than 3 wt%) and preventing the erosion of sulfate ions.

Furthermore, chloride-induced reinforcement corrosion became one of the major factors affecting the durability of marine concrete. Currently, some researchers on alleviate chloride-induced corrosion are mainly focused on physics and chemistry methods [7-9]. Physics methods are to add supplementary cementious materials or nanomaterials, such as fly ash, slag, silica fume, nano SiO2, and nano Al2O3 [10-12]. Although this method can save cost, refine pore structure of concrete and alleviate chloride-induced corrosion, the strength improvement is limited and even occur shrinkage. Chemistry methods are to add chloride ion curing agent, such as anion exchange resin, Friedel's salt (FS), Kuzel's salt (KS) and LDH, which can decrease the free chloride content of the concrete [13-15], but the effect of curing chloride ion is limited. Therefore, in this paper, we add aluminum salts (mainly $Al_2(SO_4)_3$) as admixture and utilize the synergistic effect of physics and chemistry methods to improve the mechanical properties and the corrosion resistance of marine concrete. As we all known, $Al_2(SO_4)_3{\cdot}18H_2O$ is an important components of alkali-free accelerator that can promote the hydration of tricalcium silicate (C3S), producing large amounts of calcium silicate hydrate (C-S-H) and/or expansive calcium sulfoaluminates (AFt and AFm) at early hydration ages to gain a compact structure and increase early strength of cement-based. Through structural heritability, the compactness of concrete structure after hardening is guaranteed. In addition, AFt exists a physical adsorption effect on chloride ions, and AFm can chemically combine chloride ions to generate FS and KS. The synergistic effect of AFt and AFm achieve the purpose of improving the mechanical properties and durability of concrete.

2. EXPERIMENTAL PROGRAMS

2.1 MATERIALS AND MIX PROPORTIONS

High sulfate resistance Portland cement (HSRPC) was afforded by Shandong Huayin Special Cement Co., Ltd. (China, 42.5P Grade). The chemical compositions and physical properties of HSRPC were listed in **Table 1** and the particle distribution was displayed in **Fig. 1**. Aluminum salts ($Al_2(SO_4)_3{\cdot}18H_2O$) was procured from Sinopharm Group and analytical grade. The standard sand adopted in this study complies with the Chinese standard (GB/T17671-1999), with a particle size

range from 0.08 mm to 2 mm. Furthermore, laboratory tap water was used as mixing water.

Table 1 Chemical compositions and physical properties of HSRPC

		HSRPC
Chemical compositions (%)	CaO	62.17
	SiO_2	17.70
	Al_2O_3	3.68
	Fe_2O_3	4.39
	MgO	2.99
	SO_3	3.07
	K_2O	0.84
	Na_2O	0.82
	TiO_2	0.79
	LOI	3.55
Physical properties	Specific surface(m^2/kg)	376.3
	Average primary particle size	12.09 μm
Compressive strength/MPa	7d	40.47
	28d	42.23

2.2 PREPARATION OF CEMENT PASTE AND MORTAR SAMPLES

The water-to-cement ratio was chosen as 0.5 (W/C=0.5), and the cement-sand ratio of 1:3 (C/S=1:3). The mix proportions of cement paste and mortar specimens are presented in **Table 2**. $Al_2(SO_4)_3 \cdot 18H_2O$ (1% by weight of cement) was firstly added to the mixing water and adequately dissolved. Then the HSRPC was added into the mixing water of last step, and stirred for 60 second. Finally, the standard sands were mixed with the cement paste in a mechanical mortar mixer to obtain cement mortar. The cement mortar specimens were manufactured with the cubic module of 40×40×160 mm^3 and cured at room temperature of 20±1°C and in water curing environment.

Table 2 Mix proportions for cement paste and mortar specimens

Runs	Cement Paste		Cement Mortar			W/C	$Al_2(SO_4)_3 \cdot 18H_2O$ (% by weight of cement)	$Al_2(SO_4)_3 \cdot 18H_2O$ (g)
	Cement (g)	Water (g)	Cement (g)	Water (g)	Sand (g)			
AS0	500	250	450	225	1350	0.5	0	0
AS0.25	500	250	450	225	1350	0.5	0.25%	1.125
AS0.5	500	250	450	225	1350	0.5	0.5%	2.25
AS0.75	500	250	450	225	1350	0.5	0.75%	3.375
AS1	500	250	450	225	1350	0.5	1%	4.5

2.3 TEST METHODS

In order to investigate the effect of $Al_2(SO_4)_3 \cdot 18H_2O$ on workability, mechanical properties and durability of cement paste/mortar, the fluidity were conducted according to the procedure specified in GB/T 2419-2005 and GBT/1346-2011.

The heat of hydration cement pastes was characterized by an accurate conduction calorimeter (TAM Air, USA) at room temperature (25°C) and was recorded until 3 days to obtain the heat flow and cumulate heat curves. While SEM (FEI Tecnai F20), Bruker D8 Advance X-ray diffractometer (XRD) and differential thermal analyzer (TGA/DSCI, Swiss) was used to characterize the microstructure of cement hydration products. The same settings were maintained for all the samples to ensure consistency. During the XRD test, the diffraction angle was set in the range of from 5 to 80 degree. While the TG/DSC test temperature was from 30 ºC to 1000 ºC with nitrogen protection.

RCM test was conducted out by measuring the migration coefficient of chloride ion under laboratory conditions to simulate chloride-induced corrosion in marine environments. In this paper, the cement mortar specimens with diameter of 100 ± 1 mm, depth of 50 ± 2 mm and curing for 28-days were prepared. The cement mortar specimens were treated with the voltage, which was infliction to accelerate the penetration of chloride ions. Then, the cross section of split specimens was sprayed with 0.1 M $AgNO_3$ solution in order to observe the diffusion of chloride ion and measure the penetration depth of chloride ions (at least ten points). Further, the chloride ion migration coefficient (D_{RCM}, accurate to 0.1×10^{-12} m^2/s) can be calculated as follows [16]:

$$D_{RCM}=\frac{0.0239\times(273+T)L}{(U-2)t}\left(X_d-0.0238\sqrt{\frac{(273+T)LX_d}{U-2}}\right) \quad (1)$$

Where U is the infliction voltage (V); T represents the average of the initial and final temperature of the anodic solution (°C); L is the thickness of specimen (mm); X_d represents the average penetration depth of chloride ions (mm), accurate to 0.1 mm; and t is the test duration (h).

3. RESULTS AND DISCUSSIONS

3.1 WORKABILITY OF CEMENT PASTE

The effect on the fluidity of cement-based materials is the most basic index to evaluate admixtures. Figure. 1 illustrated the influence of $Al_2(SO_4)_3$ on the fluidity HSRPC cement paste. As can be seen, the

fluidity diameter of AS samples was slightly lower (about 125 mm) than that of AS0 samples. While with the content of $Al_2(SO_4)_3$ increasing, the fluidity diameter decreased. For instance, the fluidity diameter of AS1 samples remained at about 115 mm indicating the effect of rod-like ettringite phase on forming the early structure.

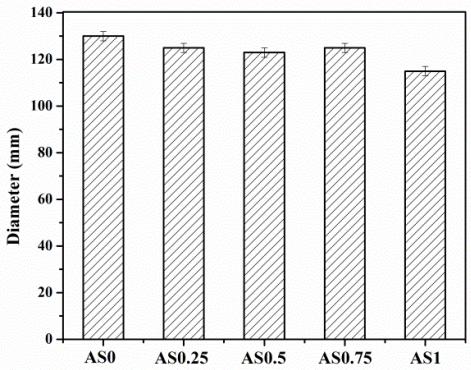

Figure. 1 Fluidity of cement pastes with various $Al_2(SO_4)_3$

3.2 HEAT OF HYDRATION

Figure. 2 depicted the heat of hydration of cement pastes with various $Al_2(SO_4)_3$. It showed that the addition of $Al_2(SO_4)_3$ did not change the hydration mode of cement pastes, but only clearly increased the reaction rate and the generated heat. And in **Figure. 2a** compared with AS0 samples, the major exothermic peaks were appeared earlier, indicating the acceleration of $Al_2(SO_4)_3$ on cement pastes hydration. This was due to the direct hydration of C3A with $Al_2(SO_4)_3$ and formed the rod-like ettringite phase. While the reaction rate slightly increased with the increasing of $Al_2(SO_4)_3$ content. **Figure. 2b** displayed the cumulative heat of cement pastes with $Al_2(SO_4)_3$ addition. The cumulative heat of $Al_2(SO_4)_3$ cement pastes was higher than AS0 samples, which was attributed to the promotion of hydration of cement paste by $Al_2(SO_4)_3$.

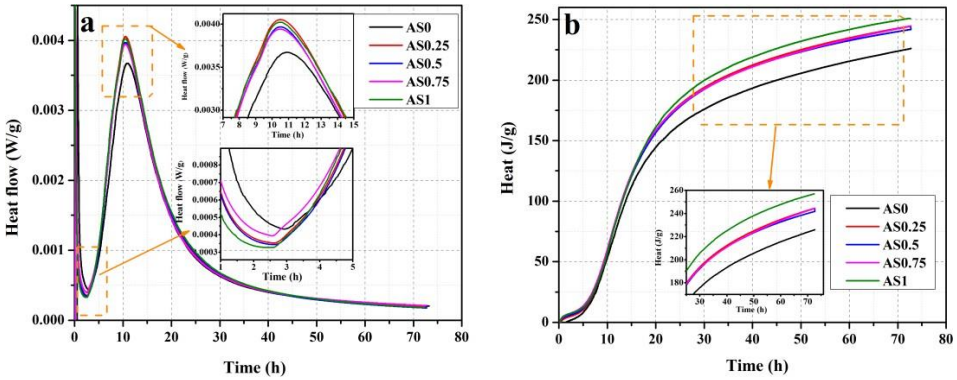

Figure. 2 Heat of hydration of cement pastes with various $Al_2(SO_4)_3$: (a) heat flow, (b) heat.

3.3 HYDRATION PRODUCTS ANALYSIS

Figure. 3 showed the hydration products analysis of cement pastes with various $Al_2(SO_4)_3$ for 3-days curing. In **Figure. 3a**, ettringite phase, $Ca(OH)_2$, alite, belite and calcite were found as the main phase. Comparing the intensity of ettringite phase, it clearly presented with the increasing of $Al_2(SO_4)_3$ content, the intensity of ettringite phase and $Ca(OH)_2$ slightly increased, indicating that $Al_2(SO_4)_3$ promoted the hydration of C3S or C3A, consumed and formed ettringite. As can be seen from **Figure. 3b and c**, there were three major peaks appeared in the DTG curves corresponding with quality loss in the TG curves, which connected to the release of water and the resolve of C-S-H, ettringite or AFm between 50 ºC and 200 ºC, the resolve of $Ca(OH)_2$ around 450 ºC-500 ºC and the resolve of $CaCO_3$ at about 680 ºC. In addition, the $Ca(OH)_2$ content was increased with 0.25% $Al_2(SO_4)_3$ compared with AS0, this was due to the effect of accelerated hydration of $Al_2(SO_4)_3$, which consisted with the XRD results.

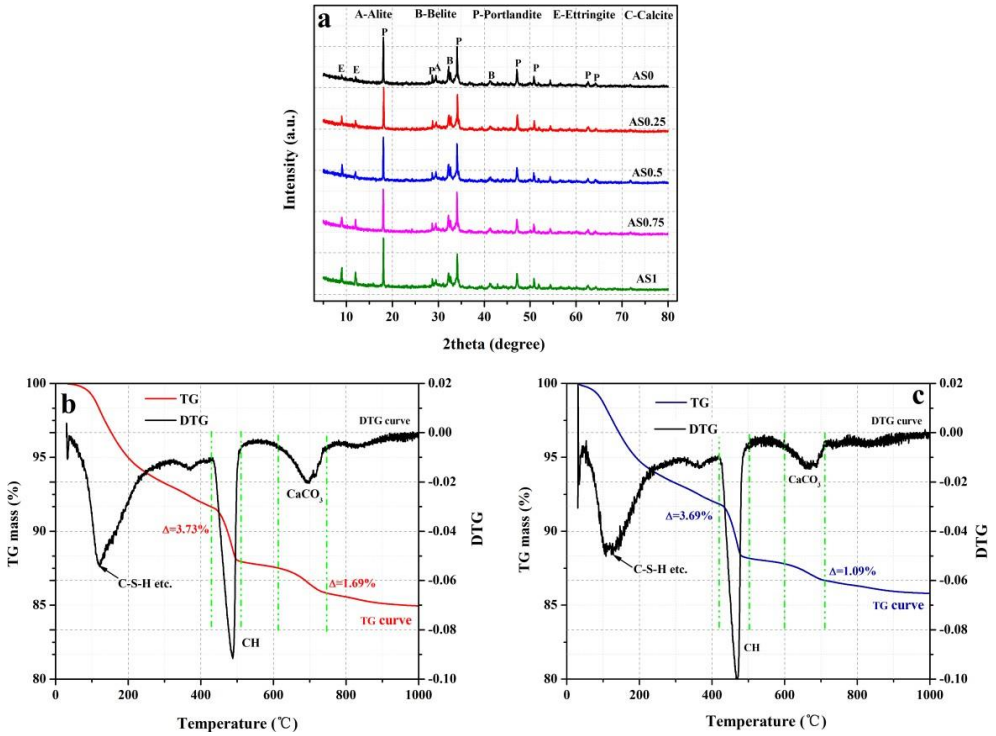

Figure. 3 Hydration products analysis of cement pastes with various $Al_2(SO_4)_3$: (a) XRD, (b) TG of AS0 samples, (c) TG of AS0.25 cement paste samples.

3.4 MICROSTRUCTURE OF CEMENT MORTAR SAMPLES

Figure. 4 described the microstructure of blank and AS0.25 cement mortar samples curing for 3-days. As can be seen, the hydration products of these two samples both contained C-S-H $Ca(OH)_2$. The connection between aggregate and cement paste in **Figure. 4a** was slightly loose and presented cracks. While from **Figure. 4b**, it can be seen that the AS0.25cement mortar samples formed rod-like ettringite phase and deposited in the pore of cement mortar, which had a certain filling effect on the pores. And there were no obvious cracks between aggregate and cement pastes. This was why cement mortar samples with AS0.25 addition had the highest compressive strength.

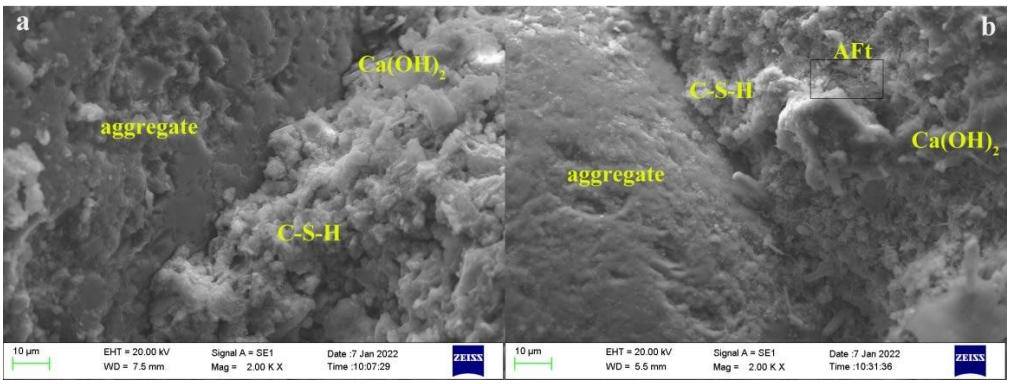

Figure. 4 Microstructure of (a) blank cement mortar samples, (b) AS0.25 cement mortar samples.

3.5 MECHANICAL PROPERTIES

Figure. 5 displayed the early-age of mechanical properties of cement mortars with various $Al_2(SO_4)_3$ after standard curing for 3-days. **Figure. 5a** showed the development of flexural strength. There was no obvious rules between $Al_2(SO_4)_3$ dosage and curing ages. This was due to the flexural strength was influenced by many factors, mainly depending on porosity and maximum pore size. It was no surprising to observe in **Figure. 5b** that the compressive strength of cement mortars with $Al_2(SO_4)_3$ addition was higher than AS0 samples and gradually decreased with the increase of $Al_2(SO_4)_3$

dosage. For instance, the compressive strength of AS0.25 cement mortars was highest (24.8% higher than AS0 samples after curing for 3-days), which was attributed to the form of rod-like ettringite phase that lead to lower porosity and higher compacted microstructure, as verified by the SEM characteristic.

In addition, the cement mortars with higher $Al_2(SO_4)_3$ addition accelerated the hydration of C3S or C3A and generated more expansive ettringite phase, which resulted in dehiscence of cement mortars and decline of compressive strength.

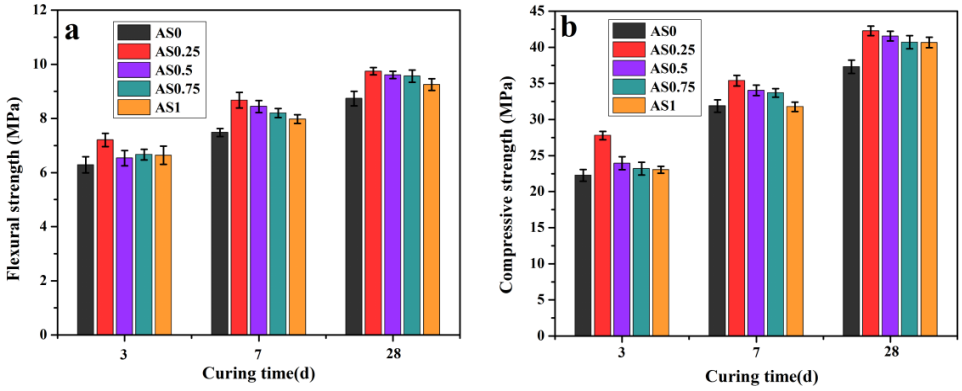

Figure. 5 Mechanical properties of cement mortars with various $Al_2(SO_4)_3$: (a) flexural strength, (b) compressive strength.

3.6 CHLORIDE ION MIGRATION COEFFICIENT

Figure. 6 showed the chloride ion migration coefficient of cement mortars with various $Al_2(SO_4)_3$, which characterized the capacity of chloride resistance. It can be seen that compared with AS0 sample, the chloride ion migration coefficient of cement mortar containing $Al_2(SO_4)_3$ was reduced to a certain extent. Among them, the AS0.25 cement mortars possessed the lowest chloride ion migration coefficient (17.52% lower than AS0 samples), this declared chloride penetration resistance was lowest due to the lower content expansive ettringite phase and more refined pore structure. Furthermore, the chloride ion migration coefficient increased with the increase of $Al_2(SO_4)_3$ content, which showed an opposite trend to the compressive strength, indicating that the higher content of $Al_2(SO_4)_3$ was disadvantaged to the chloride ion permeability resistance of cement mortar, which was attributed to the expansion caused by the generation of more ettringite and thus cracked cement mortar samples and promoted the chloride ion permeability.

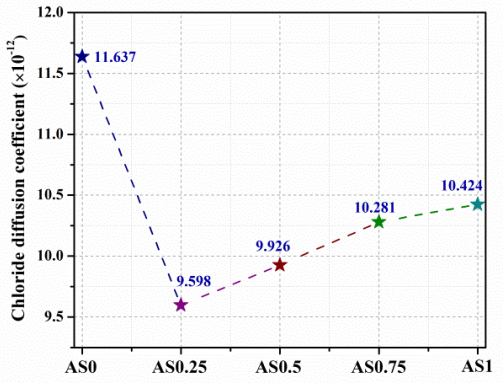

Figure. 6 Chloride ion migration coefficient of cement mortars with various $Al_2(SO_4)_3$.

4. CONCLUSION

In this paper, the essential hydration and hardened properties of high sulfate resistance Portland cement paste/mortar were investigated with $Al_2(SO_4)_3$ as admixture. A series of measurement containing fluidity, heat of hydration, XRD, TG, microstructure and RCM test were conducted. Experiment results showed that that the addition of $Al_2(SO_4)_3$ promoted the hydration of HSRP cement pastes, and the hydration rate accelerated with the increase of the addition amount. This was mainly due to the generation of ettringite, thus cement pastes quickly formed a compact hardening structure. The mechanical properties and chloride diffusion coefficient of cement mortar were obviously improved with 0.25% $Al_2(SO_4)_3$ addition. For instance, the compressive strength of AS0.25 cement mortars was 24.8% higher than AS0 samples and the chloride ion migration coefficient was 17.52% lower than AS0 samples after curing for 3-days. This may be due to the moderate addition of $Al_2(SO_4)_3$ enabled ettringite to fill the pores in cement mortar, form compact structure and blocked the chloride ion transport channel. On the contrary, excessive ettringite can cause the volume of cement mortar to expand and crack, affecting strength and durability.

ACKNOWLEDGMENTS

This work is support by the NSFC-Shandong Joint Fund Key Project (No. U1806222).

REFERENCES

1. Fodil D., Mohamed M., 2018. Compressive strength and corrosion evaluation of concretes containing

pozzolana and perlite immersed in aggressive environments. Construction and Building Materials, 179: 25-34.
2. Wang W., Lu C., 2018. Time-varying law of rebar corrosion rate in fly ash concrete. Journal of Hazardous Materials, 360(15):520–528.
3. Liu R., Jiang L.H., Huang G.H., Zhu Y.R., Liu X.R., Chu H.Q., Xiong C.S., 2016. The effect of carbonate and sulfate ions on chloride threshold level of reinforcement corrosion in mortar with/without fly ash. Construction and Building Materials, 113:90-95.
4. Demir I., Guzelkucuk S., Sevim O., 2018. Effects of sulfate on cement mortar with hybrid pozzolan substitution. Engineering Science and Technology, an International Journal, 21(3):275-283.
5. Li S., Wang S., Liu H., Bharath M.S., Zhang S., Cheng X., 2020. Variation in the sulfate attack resistance of iron rich-phosphoaluminate cement with mineral admixtures subjected to a Na_2SO_4 solution. Construction and Building Materials, 230(10):116817.
6. Chen J., Jiang M., 2009. Long-term evolution of delayed ettringite and gypsum in Portland cement mortars under sulfate erosion. Construction and Building Materials, 23(2):812-816.
7. Zahedi M., Ramezanianpour A.A., Ramezanianpour A.M., 2015. Evaluation of the mechanical properties and durability of cement mortars containing nanosilica and rice husk ash under chloride ion penetration. Construction and BuildingMaterials, 78:354-361.
8. Zhi Yeon Ting M., Soon Wong K., Ekhlasur Rahman M., Selowara Joo M., 2020. Mechanical and durability performance of marine sand and seawater concrete incorporating silicomanganese slag as coarse aggregate. Construction and Building Materials, 254:119195.
9. Mousavinejad S.H.G., Sammak M., 2021. Strength and chloride ion penetration resistance of ultra-high-performance fiber reinforced geopolymer concrete. Structures, 32:1420-1427.
10. Li L.G., Zhu J., Huang Z.H., Kwan A.K.H., Li L.J.,2017. Combined effects of micro-silica and nano-silica on durability of mortar. Construction and Building Materials, 157:337-347.
11. Farahani A., Taghaddos H., Shekarchi M., 2015. Prediction of long-term chloride diffusion in silica fume concrete in a marine environment. Cement and Concrete Composites, 59:10-17.
12. Mardani-Aghabaglou A., Sezer G.İ., Ramyar K., 2014. Comparison of fly ash, silica fume and metakaolin from mechanical properties and durability performance of mortar mixtures view point. Construction and Building Materials, 70:17- 25.
13. Yang L., Chen M., Lu Z., Huang Y., Wang J., Lu L., Cheng X., 2020. Synthesis of CaFeAl layered double hydroxides 2D nanosheets and the adsorption behavior of chloride in simulated marine concrete. Cement and Concrete Composites, 114:103817.
14. Shi C., Hu X., Wang X., Wu Z., Schutter G.d., 2017. Effects of chloride ion binding on microstructure of cement pastes. Journal of Materials in Civil Engineering. 29(1):04016183.
15. Teng Y., Liu S., Zhang Z., Xue J., Guan X., 2022. Effect of triethanolamine on the chloride binding capacity of cement paste with a high volume of fly ash. Construction and Building Materials, 315:125612.
16. Amiri A., Øye G., SjÖblem J., 2009. Influence of pH, high salinity and particle concentration on stability and rheological properties of aqueous suspensions of fumed silica. Colloid Surf A- Physicochem Eng Asp 349:43-54.